Debris and 1/*f* noise in sliding friction dynamics under wear conditions

I. Vragovic,[1] J. M. Molina,[1,2] R. Prieto,[1] M. Duarte,[1] J. Narciso,[2] and E. Louis[3]
[1]*Departamento de Física Aplicada and Instituto Universitario de Materiales, Universidad de Alicante, San Vicente del Raspeig, 03690 Alicante, Spain*
[2]*Departamento de Química Inorgánica and Instituto Universitario de Materiales, Universidad de Alicante, San Vicente del Raspeig, 03690 Alicante, Spain*
[3]*Departamento de Física Aplicada, Unidad Asociada del CSIC and Instituto Universitario de Materiales, Universidad de Alicante, San Vicente del Raspeig, 03690 Alicante, Spain*
(Received 9 July 2009; revised manuscript received 13 October 2009; published 31 December 2009)

Friction force time series showing irregular fluctuations have been since long considered one of the possible stick-slip regimes in sliding friction. However, it has not been until recently that a $1/f$ power spectrum in friction force time series derived from sliding friction experiments under wear conditions has been identified. A variety of models, mostly inspired in the field of earthquakes, has been explored, without reaching a fully satisfactory explanation of that behavior. Recently, the present authors have reported results of sliding friction experiments on steel with alumina pins, carried out with and without debris blowing, that proved the role of loose debris in determining the $1/f$ character of the friction force. A damped-forced harmonic oscillator with two friction terms was proposed to describe the dynamics of friction under wear conditions: one purely random, which accounts for surface roughness, and another inversely proportional to the amount of loose debris that was calculated by means of a modified sand-pile model. This paper presents a full discussion of the experiments that allowed to reach that conclusion and of the model proposed to rationalize the results. In addition, the results of experiments devised to understand the transition from friction with debris to friction without debris (experiment initiated without blowing and after some time switching on blowing) and vice versa are reported. The results of further studies of the wear track are presented, namely, the variation in the track width with sliding distance and results of chemical analyses and surface roughness measurements of the track, for both with or without debris blowing experiments. These additional data give further support to the crucial role of debris in the $1/f$ character of the friction force.

DOI: 10.1103/PhysRevE.80.066123 PACS number(s): 62.20.Qp, 89.20.Kk, 46.55.+d, 05.40.−a

I. INTRODUCTION

Wear and friction are two phenomena, concomitant in many systems, that have a great economical and technological importance [1–3]. Both, and particularly wear, are among the most difficult and less understood issues in materials science. The very rich phenomenology that characterizes wear is precluding the development of a theoretical framework having general applicability. For instance, evaluating wear depends on the type of experiment and the counterpart material to such an extent that most industrial laboratories do evaluate wear performance exactly under the same conditions of the application for which the material was devised.

Depending, among other factors, on the sliding speed and the elastic properties of the experimental device, three regimes have been identified in sliding dynamics [1]: (i) a steady regime characterized by a constant friction force, (ii) a stick-slip regime, in which the friction force varies periodically with time, and (iii) stick slip with a friction force showing irregular fluctuations. Experimental studies indicate that whereas regime (ii) shows up whenever wear effects are weak [4], regime (iii) has been observed in several systems having in common the presence of strong wear effects [5–9]. In the latter experiments, it was observed that the power spectrum of the friction force time series was self-similar and had a $1/f$ character [5–8]. Irregular stick slip has also been observed in lubricated sliding friction; in this case, the system may enter into what is called a "granular sliding state" (see Ref. [1]).

In spite of the various features that friction and wear share with earthquakes phenomena, in which self-organized criticality and $1/f$ noise had been identified [10], earlier theoretical or numerical analyses of this issue triggered a vivid debate [11,12]. On the other hand, in order to describe both high- and low-frequency regions of the friction force power spectrum, it was proposed to combine a Tomlinson-like and a modified Robin Hood model [6] (the Robin Hood model of self-organized criticality was originally proposed for dislocation motion; see Ref. [13]). None of these models, however, incorporates a key ingredient in sliding friction under wear conditions, namely, the great amounts of debris being generated at the contact area. The role of debris in sliding friction is well documented [3,14–18]. Depending on the system at hand, debris may favor plowing of the worn surface, thus, increasing the friction coefficient [15], or form a protective tribolayer [3,15–18] that decreases friction and subsequently wear. Moreover, if debris are loose [17], they may act as a fluidized bed that also reduces friction. These effects are usually concomitant, and, which of them predominates, depends on the type, morphology, and size of debris.

Recently, the present authors have investigated the effects of debris on the power spectrum of the friction force time series. To this end, they carried out dry sliding friction experiments on a pin-on-disk equipment with or without blowing debris. Due to the characteristics of the experimental setup, the sample material (steel) and the pin material (alumina spheres), wear effects were strong and debris (oxidized iron particles) were mostly loose. The results unambiguously

showed that *loose debris are determinant in what concerns the* $1/f$ character of the friction force. The aim of the present paper is to discuss in depth the experimental results that support this conclusion and the model used to describe the dynamics of this system.

The rest of the paper is organized as follows. Section II is devoted to describe the materials and the experimental procedures. In particular, the sliding friction experiments are described in Sec. II A, while the important issue of data analysis is dealt with in Sec. II B. The following section is devoted to the model used to analyze the experimental results. First, in Sec. III A, the dynamical equation is discussed while the sand-pile model used to calculate the amount of debris versus time is described in some detail in Sec. III B; finally, the role played by each parameter of the model is briefly commented on in Sec. III C. Section IV is devoted to the results, starting with the core of this work, namely, the experimental evidence of a $1/f$ character of the friction force time series in sliding friction experiments under strong wear conditions and the model used to rationalize the results (Sec. IV A). Results for the average friction force and the wear track produced with or without debris blowing are discussed in detail in Sec. IV B. Section IV ends with a discussion of additional experiments that provide further support to the main argument of the present work. The last section gathers the main conclusions that can be drawn from the results presented here.

II. MATERIALS AND EXPERIMENTAL PROCEDURES

A. Slide friction experiments

Dry friction experiments were carried out in a CSEM Instruments pin-on-disk tribometer built according to the ASTM G99 standard. A photograph of the instrument and a schematic view of the load arm that holds the pin are shown in Fig. 1. The spring constant of the apparatus was determined by measuring the pin displacement upon hanging a given weight, resulting $k=63$ kN/m. A fitting of the experimental data for displacement versus load is shown in Fig. 2(a). Dynamic measurements (oscillations of the pin after having been displaced from the equilibrium position) allowed to measure the apparatus normal frequency $\omega_0 = 92$ rad/s and estimate the average value of the damping constant $b=65$ Ns/m. As can be noted in Fig. 2(b), although at short times the oscillatory behavior may depend on the initial displacement, the two curves shown in the figure soon become very similar. In addition, their Fourier transforms (FTs) give the same predominant frequency, although of course the spectrum has many other frequencies with non-negligible weight.

The material used in the experiments was steel SAE 52100. Samples of 20 mm in diameter and 5 mm thick were cut from commercial rods, polished (grinded) with silicon carbide paper up to 400 mesh, and cleaned in an acetone ultrasonic bath. Care was taken to ensure good surface finishing (see Appendix B) and that the two disk faces were parallel. Alumina pins (spheres) 6 mm in diameter were used all throughout. The sample, in contact with the alumina pin, rotates at a fixed speed producing a wear track of average

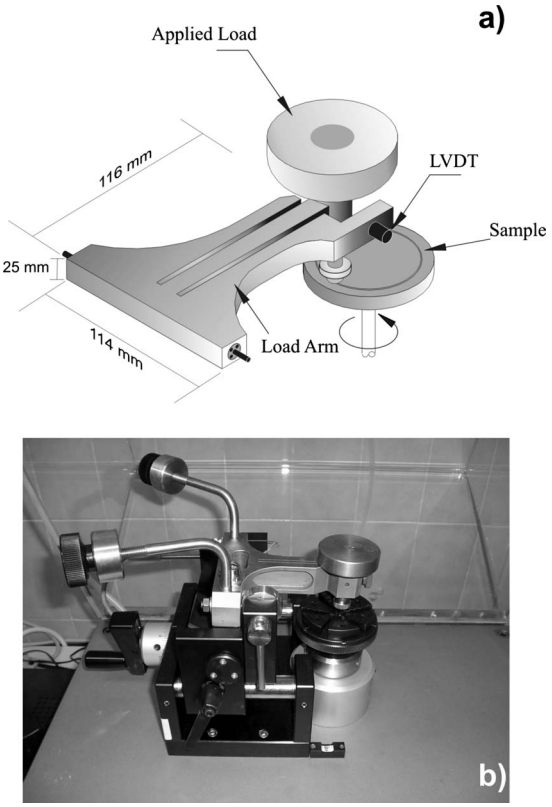

FIG. 1. Schematic view of the load arm (a) and photograph (b) of the pin-on-disk tribometer used in this work (LVDT stands for linear variable differential transformer).

radius 0.5 cm (this can actually be varied, but it was kept fixed in the present experiments).

The friction force versus time $F(t)$ was recorded using a data acquisition (DAQ) card controlled by LABVIEW. Experiments were carried out at applied loads Q in the range 2–10 N and sliding speeds ranging from 0.05 up to 25 cm/s, and without or with debris blowing. The latter was done by means of a synthetic air jet (20% O_2, 80% N_2, water ≤ 3 ppm, and hydrocarbons ≤ 0.1 ppm). Typical friction force time series obtained without and with debris blowing are depicted in Fig. 3.

Debris produced during the experiments were examined visually and by means of scanning electron microscopy. Almost all debris appeared to be oxidized (showing the typical reddish color of iron oxides), as confirmed by means of energy dispersive x-ray analysis (EDX). No appreciable agglomeration was observed, most of the wear debris being loose, as illustrated in Fig. 4.

B. Data analysis

As several studies indicate that $1/f$ noise is a low-frequency effect [19], long-distance experiments were carried out to go as far as possible into the low-frequency region of the spectrum. In order to attain long enough distances, data were taken in most cases at 20 Hz. It was checked that no relevant events occurred beyond this frequency. Anyhow, some checking of the high-frequency end of the spectrum

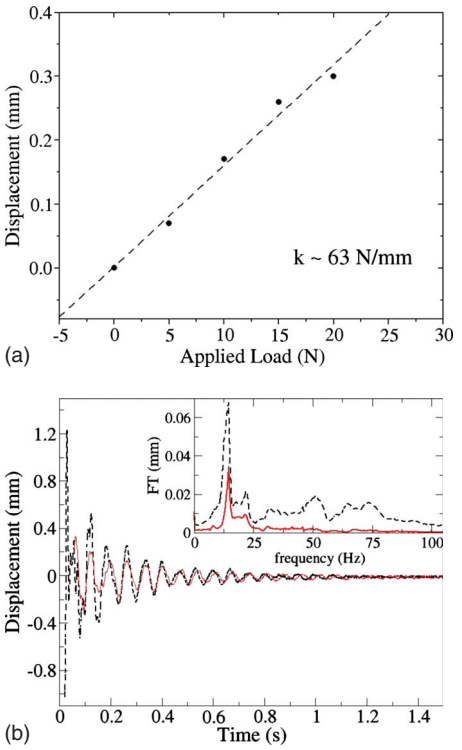

FIG. 2. (Color online) (a) Determination of the spring constant k of the tribometer. (b) Results of two typical dynamical experiments addressed to determine the normal frequency and the damping constant of the tribometer. Inset: Fourier transform of the displacement versus time series from which a predominant (normal) frequency was derived, namely, $\omega_0 = 92$ rad/s.

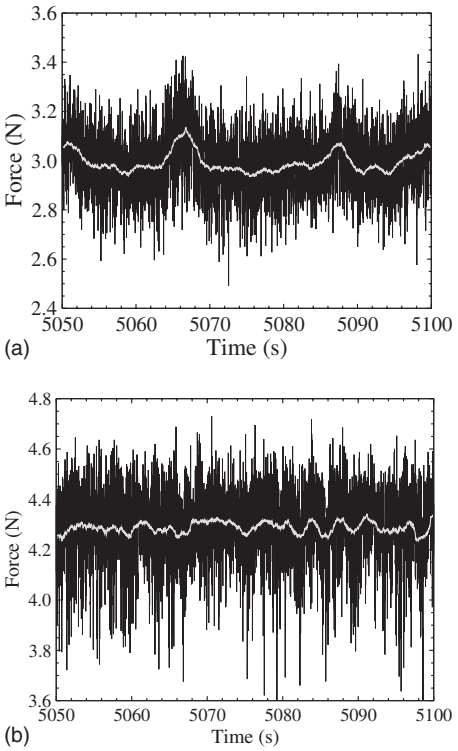

FIG. 3. Friction force vs time derived from sliding friction experiments on SAE 52100 steel with an alumina pin, carried out at a load of 10 N and a speed of 1 cm/s without (a) and with (b) debris blowing.

was done recording data at 1 KHz. Several runs carried out without pin/sample contact allowed to check that internal fluctuations had much smaller amplitude than the friction force (at least a factor of 20 smaller) in any of the experiments discussed in this work. This is illustrated in Fig. 5, where the signal provided by the tribometer with no pin/sample contact and with and without air blowing is depicted.

Only data recorded beyond the transient, the time interval required to initiate the wear track and over which the friction force varies abruptly, were used to derive the power spectrum. The recorded data set was analyzed either as a whole (sets containing up to three million points were commonly used) by means of discrete Fourier transform (DFT) or in batches so that the amount of data used in applying fast Fourier transform algorithms was always an exact power of 2 (actual batches varied from 2^{19} to 2^{21} data points) from which an average power spectra were subsequently obtained. In general, DFT was preferred as it did not put any limitation on the batch size. Although most of the power spectra discussed below were obtained by means of DFT of data sets containing around three million points, it was in some cases checked that both procedures led to similar results.

III. MODELING SLIDE FRICTION UNDER WEAR CONDITIONS

A. Dynamic equation

Our basic assumption is that the position of the pin as a function of time $x(t)$ (the magnitude actually measured in the experiment) is governed by the equation of motion of a damped and forced harmonic oscillator,

$$\frac{k}{\omega_0^2}\frac{d^2x(t)}{dt^2} + b\frac{dx(t)}{dt} + \omega_0^2 x(t) = F(t). \tag{1}$$

In the absence of the external force $F(t)=0$, this equation described a damped harmonic oscillator that should correspond well to the pin/apparatus system without contact with the rotating sample, having an elastic constant k, a normal-mode frequency ω_0, and a damping constant b (all three measured as described in the preceding section). We suppose that

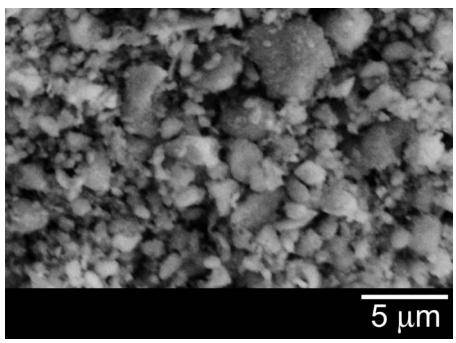

FIG. 4. SEM micrograph of the wear debris produced in the sliding friction experiments carried out in this work. Debris show the reddish color (not visible in the figure) typical of iron oxide, and its size varies over the range 1–20 μm.

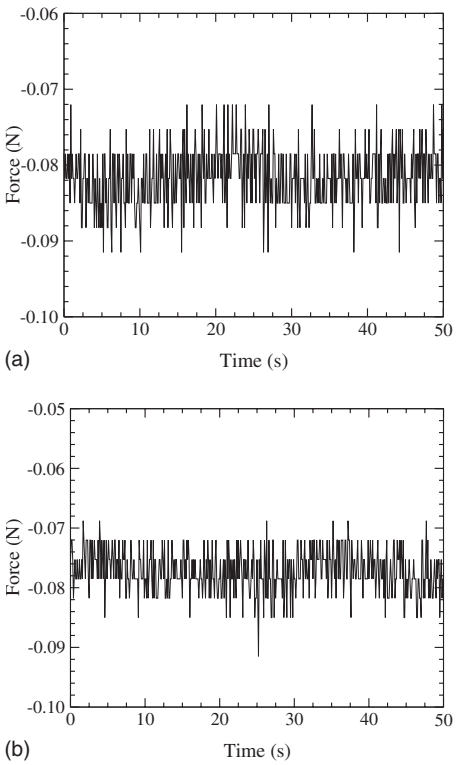

FIG. 5. Signal obtained without pin/sample contact, without (a) and with air blowing (b).

the friction force $F(t)$, originating from the pin/sample contact, has two terms. The first term is related to the effect of debris forming a lubricating layer and is assumed to be inversely proportional to the amount of debris, while the second accounts for the random profile of the surface of the rotating sample. Then, the friction force is written as

$$F(t) = -\operatorname{sign}\left(\frac{dx(t)}{dt}\right)\left[(1-p)\frac{f_A}{D(t)} + p(f_B + \sigma\epsilon)\right], \quad (2)$$

where $D(t)$ is the total amount of material (debris) on the pin/sample contact area at time t; f_A and f_B are model parameters; ϵ is a random Gaussian variable whose amplitude is denoted by σ; and, finally, $p \in [0,1]$ is the contribution of the random profile. Thus, the model has three constants characteristic of the apparatus used to carry out wear experiments (k, ω_0, and b) and four model parameters (f_A, f_B, σ, and p). In addition, a procedure to calculate $D(t)$ has to be proposed. Here we use the sand-pile-like model described below that we believe to be adequate for the present case. The specific values of the just-mentioned model parameters plus those related to the sand-pile model (see below) were chosen to reproduce the measured values of the friction force and of the $1/f$ exponent and will be given in Sec. IV.

B. Amount of debris versus time: A sand-pile model

We attempt to simulate the generation and elimination of debris along the experiment $D(t)$ using a simple cellular automata that can be classified within the framework of sand-pile models [20–23]. Our choice is a local model having the critical slope as the ordering parameter (i.e., there is no explicit limit on the amount of grains per cell). In order to avoid formation of a single hill of material that is characteristic of systems with open boundaries, cells are arranged into a two-dimensional (2D) square lattice with periodic boundary conditions that has a number of drain cells through which material is lost (see below). We start the simulation taking $D(0)=0$. Then, at each time step, we add a fixed amount of grains η into one randomly choosen cell updating its amount of grains (i.e., its height h),

$$h(i,j) = h(i,j) + \eta. \quad (3)$$

After the addition, a set of rules is applied, checking whether the slope between the chosen cell and some of its neighbors is large enough to initiate the redistribution of the material and the relaxation of the whole system into a new stable state. The excess of material is lost through a number of drain cells N_{dc} proportional to the size of the system, through which material is removed at a given rate. The positions of drain cells are updated randomly after τ time steps, causing quite irregular profile of movable hills and valleys within the system. The drain cells may account for debris sticking on the surface, a process that occurs along the experiments (see below). Debris losses may also occur through boundaries of the pin/sample contact area, although here this is precluded by our assumption of periodic (instead of open) boundary conditions.

Contrary to other 2D approaches, we define the slope simply as the height difference between a reference cell (i,j) and each of its four nearest neighbors [20,21]

$$\Delta h(i,j|i+1,j) = h(i,j) - h(i+1,j) \quad (4)$$

and similarly for $(i-1,j)$, $(i,j+1)$ and $(i,j-1)$. Once the critical slope between two neighboring cells is reached, we start the relaxation process having its internal time scale. We suppose that the relaxation process is much faster than the addition of new material. Thus, from the viewpoint of measurement of the position of the pin, the redistribution process appears to be instantaneous. We check the slopes between the reference cell and its four neighbors and choose the most unstable one. In the case that several unstable slopes have the same value, we pick up one of them at random. Then some amount of material (δ) is moved from the higher to the lower hill, where $\delta \leq \Delta h_{\max}/2$,

$$h(i,j) = h(i,j) - \delta,$$

$$h(\text{neighbor}) = h(\text{neighbor}) + \delta. \quad (5)$$

The redistribution continues at each step of the internal time scale of the relaxation process until the system reaches a new equilibrium. The final amount of material thus obtained is used as an input value for the calculation of the macroscopic friction force at that particular time.

C. Role of the model parameters

The amount of grains per cell within the 2D lattice depends on the model assumptions and the values given to the model parameters. It has no direct physical meaning but

should be reflected into the amount of material (loose debris) accumulated between the pin and the disk. In order to obtain a physically meaningful magnitude, we multiply $1/D(t)$ by a suitable parameter f_A estimated in accordance with the measured values of the macroscopic friction force. As remarked above, taking one of the contributions to the friction force to be inversely proportional to the amount of debris $f_A/D(t)$ is based upon the fact that loose debris may act as a lubricant, thus, decreasing friction. Parameters f_A, f_B, and σ take different values for each particular experiment (with or without blowing, load, speed, etc.) in order to reproduce the measured friction force $F(t)$ and the amplitude of its fluctuations. In addition, we specify the contribution of the random profile of the sample surface by choosing an appropriate value for $p \in [0,1]$; in particular, we chose $p=0.05$, a value that gives the correct slope of the Fourier-transformed curve of the measured friction force time series. This indicates that about 95% of the total friction force originates in the layer of loose debris.

Finally, we address what are the optimal values for the parameters used in the sand-pile model. When choosing the size of the lattice $(L \times L)$, we should set it large enough to permit the microscopic redistribution mechanism of the sand-pile model to take place and to get better resolution for small variations in the number of grains per cell as a function of time. However, on the upper side, the size of the lattice should be small enough to allow numerical calculations to be performed within a reasonable limited time. The critical slope $(\Delta h_{\max})$ should be small enough to shorten the transient period of the initial accumulation of material before the redistribution starts and large enough to permit noticeable differences between the amounts of grains in different cells. The amount of transferred material (δ) must be less or equal to the half of the critical slope. For $\delta=\Delta h/2$, two neighboring cells would have the same amount of grains after the redistribution. The number of drain cells (N_{dc}) is arbitrary and proportional to the size of the system. As we have seen, the amount of grains per cell $D(t)$ depends mainly on Δh and δ. However, the particular values it takes do not really matter, as it should be rescaled later by the factor f_A in order to reproduce actual values of the measured macroscopic friction force $[F \sim f_A/D(t)]$. As already remarked, the applicability of the model is actually checked by comparing the slope of the transformed curve of the model time series with the measured one.

IV. RESULTS

A. Effect of debris on the 1/f character of the friction force time series: Experiments and modeling

Experimental results for the friction force time series without and with debris blowing are shown in Figs. 3(a) and 3(b), respectively. Raw data are plotted to avoid any biasing. It is first noted that the friction force is higher when debris are removed (average around 4.2 N to be compared with 3 N in the experiment without blowing). Fluctuations are also appreciably stronger in the latter case. Although running averages also shown in the figures indicate some differences in the inner structure of the two time series, the effects of blowing are in this case not apparent. Remarkable differences do instead emerge upon Fourier transforming, as the results of Figs. 6(a) and 6(b) clearly indicate. At frequencies higher than 0.1 Hz, both FTs show similar noisy patterns. In particular, the FT of the time series derived from experiments without blowing shows a series of sharp peaks starting at 0.318 Hz (see Fig. 6): a frequency which coincides with the inverse of the time needed to complete a full rotation at the speed at which those experiments were carried out (1 cm/s). It was checked that the subsequent peaks are the harmonics of that frequency. As suggested in Ref. [8], this peak series is probably due to sample nonhorizontality. Blowing distorts this simple picture [see Fig. 6(b)], and the frequencies at which the peaks show up cannot be derived from such a simple reasoning. An outstanding feature common to both cases (with or without blowing) is the flattening of the spectrum at high frequencies, an effect that finds a sound and simple explanation within the framework of the model proposed here (see below). Other effects, such as aliasing, may also pollute the high-frequency end of the spectrum [8].

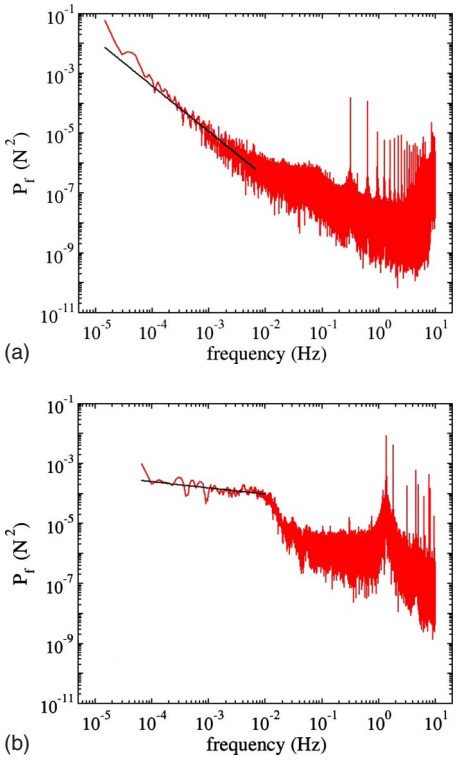

FIG. 6. (Color online) Power spectra of the friction force time series derived from sliding friction experiments on SAE 52100 steel with an alumina pin, carried out at a load of 10 N and a speed of 1 cm/s, and without and with debris blowing [(a) and (b), respectively]. The discrete Fourier transform was done over sets containing 3×10^6 data points. The straight lines are least-square fits of a power law $P_f \propto f^{-\beta}$, with $\beta=1.53$ without removal of debris (a), and $\beta=0.2$ when debris are blown away (b). As compared to the results shown in Fig. 1 of Ref. [9], here a running average every three points was done; this average, albeit smooths the curves, affects only marginally to the exponent β.

Having taken note of this and recalling the fact that $1/f$ noise is a low-frequency effect, we concentrate on the region

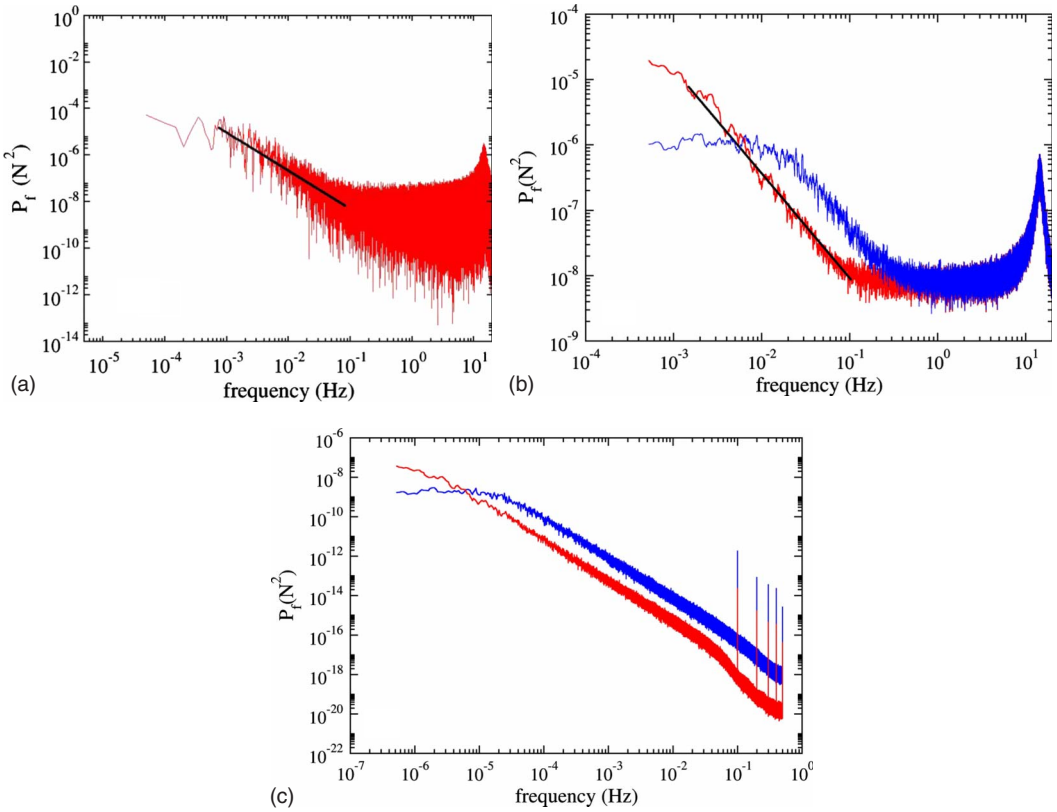

FIG. 7. (Color online) [(a) and (b)] Power spectra (in N^2) of the friction force time series derived from the model proposed here to describe the effects of debris. The discrete Fourier transform was done over sets containing 20×10^6 data points. Raw data (a) and running averages over 20 points of DFT data (b) are shown. The results correspond to simulations carried out on clusters of the square lattice with periodic boundary conditions of sizes 32×32 (blue broken curve) and 100×100 [red continuous curve and (a)], respectively. The exponent obtained in the latter case for a fitting over the range $2\times10^{-3}-10^{-1}$ (black continuous straight line) is −1.64. (c) Power spectra (in N^2) of the inverse of the amount of debris versus time $1/D(t)$ as derived from the sand-pile model described in the text. The exponent obtained for a power-law fitting over the range $2\times10^{-3}-10^{-1}$ is −1.83.

of the spectrum below 0.01 Hz. At low frequencies, the friction force time series derived from experiments carried out without removing debris shows a power spectrum that admits a power-law fitting over a range covering at least three decades [from approximately 7×10^{-6} up to 7×10^{-3} Hz; see Fig. 6(a)]. This is an unambiguous signature of a $1/f$ spectrum. In turn, removing debris takes out to a great extent all signs of $1/f$ behavior, leading to a power spectrum that does not admit a reasonable power-law fitting. However, if one insists in doing such a fit, it is feasible over a range covering around two decades [see Fig. 6(b)] but with an exponent of −0.23 to be compared with the exponent −1.58 found in the case without debris removal (see caption of Fig. 6). Such a low exponent is closer to white noise than to standard $1/f$ behavior.

Figure 7 shows results derived from the model described in the preceding section. The values of physical magnitudes and parameters used to generate those results are the following: (i) the three constants of the experimental apparatus $k=59$ kN/m, $\omega_0=92$ rad/s, and $b=65$ Ns/m and (ii) the four parameters in the equation of motion $f_A=22$ N, $f_B=4$ N, $\sigma=4$ N, and $p=0.05$. We calculated the amount of debris versus time carrying out numerical simulations on $L\times L$ clusters of the square lattice with periodic boundary conditions (where L is given in units of the lattice constant). The parameters used in the simulations were chosen to reproduce the measured values of the friction force and of the actual $1/f$ exponent: (i) the critical slope $\Delta h_{\max}=6$, (ii) the transfer of material $\delta=2$ (this was also taken to be the rate at which material was removed through the drain cells), (iii) the amount of grains added during each time step $\eta=1$ or 10 for $L=32$ or 100, respectively, and (iv) the number of drain cells $N_{dc}=1$ or 10 for $L=32$ or 100, respectively. The positions of the drain cells were updated after $\tau=10$ steps. In order to compare simulations with experiments, we have assumed that each Monte Carlo step corresponds to 1 ms.

The time series derived from the adopted model has a pattern similar to the experimental series (see Ref. [9]). On the other hand, its Fourier transform shows a well-defined $1/f$ character over at least two decades, as the results reported in Fig. 7 clearly indicate. It is noted that running averages in Fig. 7(b) reveal more clearly the power law than the raw data of Fig. 7(a). As the results for $L=100$ depicted in Fig. 7 show, the power spectrum of the simulated friction force time series (containing $p=5\%$ of white noise) has $1/f$ behavior with an exponent of −1.61. On the other hand, reducing the white noise to zero, the resulting exponent is within the range $[-1.8,-2]$ (depending on the frequency range over which the fitting is carried out), significantly larger than the one reported to be the most accurate for the

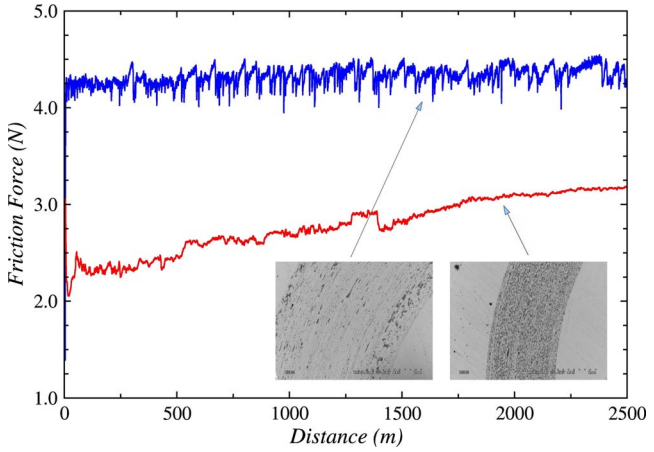

FIG. 8. (Color online) Running averages of the friction force vs time derived from experiments carried out on SAE 52100 steel with an alumina pin at a load of 5 N and a sliding speed of 10 cm /s. Data were taken at 20 Hz and averages were done over successive ranges of 50 s. Experiments carried out with (green upper curve) and without (red lower curve) debris blowing. Wear tracks micrographs are also shown.

standard sand-pile model in two dimensions, namely, −1.59 [20,23] [see Fig. 7(c)] and larger than the measured one. The frequency range covered by the power-law fit depends on the cluster size L. For a cluster with $32\times32=1024$ cells, which range extends from 10^{-2} Hz to 1 Hz, while for lower frequencies we got rather flat spectra (see Fig. 7). On the contrary, in the case of the larger 100×100 cluster, a well-defined power law appears at lower frequencies, covering slightly more than two decades. Thus, the flattening of the spectrum in the low-frequency region surely is a size effect. At high frequencies, however, the spectrum is dominated by the friction force related to surface randomness, which produces a white-noise response, offering a reasonable explanation to the flattening observed in the experimental FT (see Fig. 6). Actually, the power spectrum of the inverse of the amount of debris $1/D(t)$ (without any white noise added) follows a steeper power law up to the high-frequency end (see Fig. 7). Finally, the distinct peak slightly above 10 Hz corresponds to the natural frequency of the tribometer.

B. Average friction force and the wear track

Running averages of the friction force are shown in Fig. 8. The first significant feature to be noted is the much larger friction force obtained when debris are removed. This is due to the lubricating role that a layer of mobile debris plays. In addition, when debris are removed, the friction force increases abruptly at the beginning remaining constant thereafter (fluctuations to be discussed later), whereas in the case without debris removal the friction force remains increasing slowly up to rather long times. This apparent difference can be rationalized by noting that the roughness of the wear track in the latter case increases along the experiment (see Fig. 8) due to sticking of debris onto the sample surface, an effect which is much weaker in the case of debris removal. Increasing the surface roughness produces a reduction in the mobility of the debris layer, thus, increasing friction. Fluctuations that survive the average process are significantly larger in the case of debris removal probably due to the shock absorber role played by debris. Finally, note the large difference between the wear tracks in the two cases, being wider and "cleaner" when debris are removed in accordance with stronger wear effects. In deep track, debris may accumulate close to the track walls, an effect that can be easily identified in Fig. 8 (see also Appendix B).

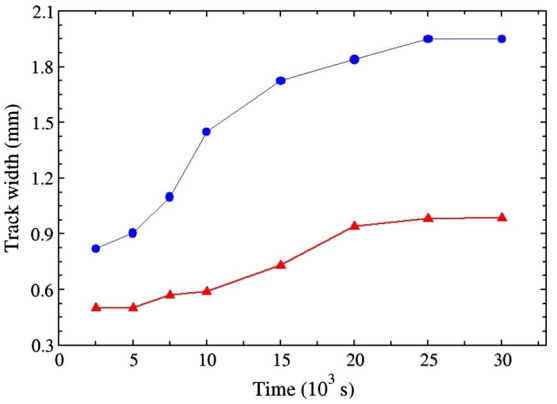

FIG. 9. (Color online) Track width versus sliding time derived from experiments carried out on SAE 52100 steel with an alumina pin at a load of 5 N and a sliding speed of 10 cm /s. Data were taken at 20 Hz. Experiments were carried out with (circles) and without (triangles) debris blowing.

As noted in the preceding paragraph, the track is wider in the experiment with blowing. We have quantified this difference by measuring the wear track width versus sliding time in experiments carried out with or without debris blowing. The results are depicted in Fig. 9. The track in case debris are blown is approximately twice wider than in the experiment without blowing. In addition, the stationary state (track width approximately constant therein) is reached earlier in the first case; this implies a steeper increase in width at the beginning of the experiment with debris blowing). These results are all compatible with the main effect that debris produce, namely, reducing wear.

C. Additional experiments

In order to further illustrate the role of the fluidized debris layer and its characteristics, two experiments initiated without debris removal were stopped and debris removed either by blowing or by applying ultrasounds. Both were subsequently reinitiated. The results are shown in Fig. 10. In both cases, the friction force drops upon debris removal. This result, at first sight in contradiction with the main assumption of this work, can be rationalized by noting the significant increase in surface roughness promoted by debris sticking along the whole experiment. When debris are removed, the shock absorber effect is eliminated, an effect that seems overcompensated by the reduction in the pin/sample contact area due to debris sticking, and, consequently, the friction force. Thereafter, the friction force recovers the value it had before the experiment was stopped. It is also interesting to

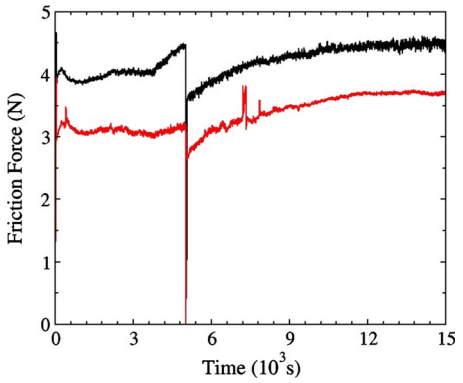

FIG. 10. (Color online) Friction force vs time derived from experiments carried out on SAE 52100 steel with an alumina pin at a load of 5 N and a sliding speed of 10 cm /s. Data were taken at 20 Hz and averages were done over successive ranges of 50 s. Experiments were carried out without debris blowing stopped after 5000 s and debris removed either by blowing (red line) or in an ultrasound bath (black line, displaced 1 N upward) and reinitiated thereafter. Fluctuations have an amplitude smaller than in Fig. 2, as some filtering in catching the data was used.

note that this drop is only slightly larger in the case of ultrasound removal, indicating that debris were either loose or strongly stuck onto the wear track.

Two additional experiments that may throw light on the dynamics of track formation were carried out. The first was initiated without blowing and after the system entered into the stationary regime, blowing was switched on. In the second just the opposite was done, namely, it was started with debris blowing and, after a while, blowing was switched off. The results are reported in Fig. 11. The most striking difference is the duration of the transient, very short in the case blowing-no blowing and long in the other experiment. This is consistent with all results discussed in this work, in the sense that in the absence of debris wear is much stronger sharply reducing the transient period. In addition, while in the blowing-no blowing experiment the friction force reaches the value that was attained in the standard experiment with blowing (around 4.5 N), in the second experiment the friction force saturates at 3.6 N, somewhat larger than in the standard experiment with blowing. This result is without doubts a consequence of the wider track produced during the blowing stage.

V. CONCLUSIONS

In this work, we present a detailed discussion of the experimental results previously published by the authors [9], which indicate that debris are determinant in what concerns the $1/f$ character of the friction force observed whenever sliding friction occurs under strong wear conditions and the produced debris are loose. The model proposed by the authors to rationalize these results is here described in detail. In particular, a considerable attention is devoted to the modified sand-pile model used to describe the fluidized layer of debris between the sample and the pin. Emphasis is placed on the fact that the model allows to relate the flat spectrum at high

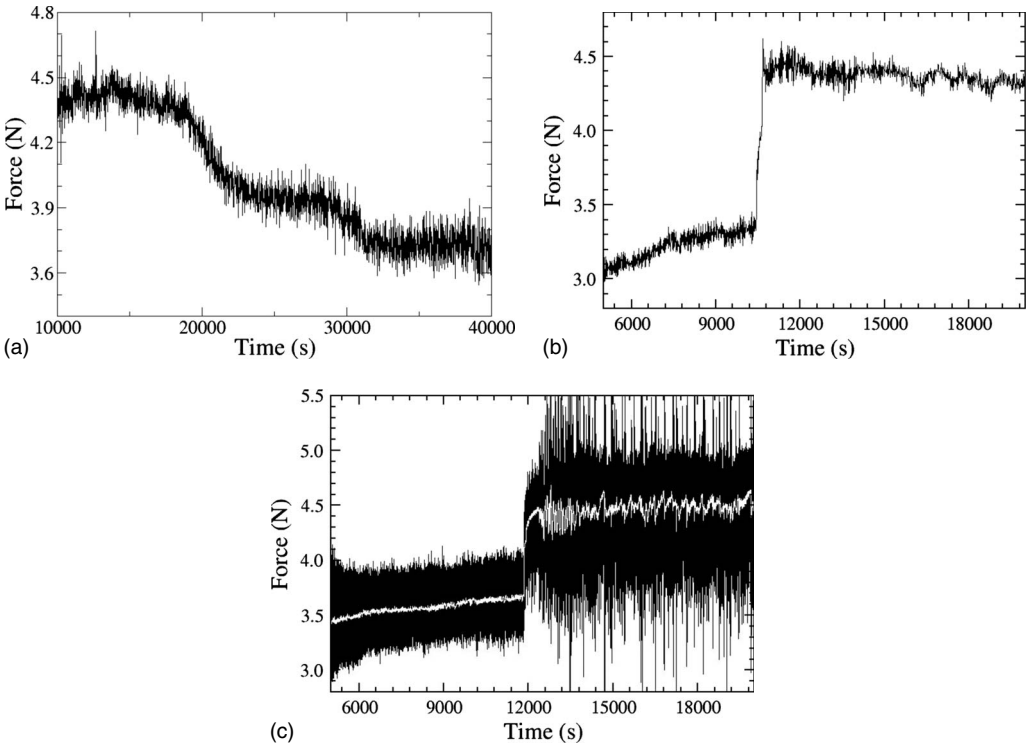

FIG. 11. Results for the friction force vs time derived from an experiment, in which initially debris were not blown and, after the force was roughly stabilized, blowing was switched on (a) and vice versa (b). In the latter case, results obtained in another experiment, in which no electronic filtering was used, are also shown (c), along with a running average (white curve). Experiment carried out on SAE 52100 steel with an alumina pin at a load of 5 N and a sliding speed of 10 cm /s. Data were taken at 20 Hz.

frequencies derived from the experiments to surface roughness, while the 1/*f* character at low frequencies is explained in terms of the fluidized bed built up by loose debris. Results for the wear track width show that it is actually much larger in the experiments with blowing (twice that obtained in the experiments without blowing), in line with the higher average friction force observed in that case. Chemical analyses and visual observation of debris unambiguously indicate that they are iron oxides. Surface roughness measurements reinforce the interpretation of the experimental results discussed in this work.

As the phenomenology related to wear is very rich, the results discussed here (the 1/*f* character of the friction force included) may not have a general validity. In particular, two conditions have to be fulfilled: friction occurring under strong wear conditions and wear debris be mostly loose.

ACKNOWLEDGMENTS

Thanks are due to the Spanish Ministerio de Educación y Cultura (Grant No. MAT2005-03139) for partial financial support. We thank C. García-Cordovilla and S. Marcilla for useful discussions on surface roughness. M.D. and R.P. acknowledge grants from the ADEMAT (Advanced Engineering Materials) Network (E.U. Project No. II-0240-B1-AT-RT-CT).

APPENDIX A: SEM AND EDX ANALYSIS OF DEBRIS AND TRACK

We have carried out extensive scanning electron microscope (SEM) and EDX analyses of the wear debris and the wear track. As remarked above, debris are mostly loose. Chemical compositions of light and dark zones of the wear track (see Fig. 8) taken after 2000 m testing with or without blowing are reported in Table I. Although, unfortunately, it was not possible to obtain quantitative results for debris, EDX allowed to unambiguously detect the presence of both Fe and O. This qualitative result, along with its reddish color, clearly indicate that they are mostly iron oxides. As discussed in the main text, the SEM micrographs of the wear track (see Fig. 8) clearly reveal that the track without blowing is full of small black regions, which, as indicated by the EDX results, probably are iron oxides. The gray areas are mostly free of oxygen. Blowing mostly eliminates the black areas, although some are visible at the edges of the track. The reason for this effect is that after such long testing, the track is rather deep and, consequently, blowing accumulates debris in the outer edge. In the inner edge, some dark spots (particles) are also seen due to the fact that injected air may not reach that zone when the track is deep. EDX reveals that, as in the case without blowing, dark regions contain oxygen and light regions do not.

TABLE I. Chemical composition (in at. %) in light and dark zones (LZ and DZ, respectively) of the wear track produced in sliding friction experiments with and without blowing. Errors are given in parenthesis.

Blowing	Zone	Co	Fe	O
YES	LZ	1.38 (0.1%)	96 (2.9%)	2.96 (0.5%)
	DZ	0.68 (0.1%)	58 (2.4%)	41 (3.6%)
NO	LZ	1.06 (0.1%)	78 (2.6%)	20.8 (1.8%)
	DZ	0.54 (0.1%)	45 (2.1%)	54 (5%)

Quantitative results obtained at 20 keV are reported in Table I. Data have to be taken with caution as the various regions are difficult to resolve (mainly due to the limited spatial resolution of EDX). In the dark regions of the wear track produced either with or without blowing, the ratio of atomic percentages of Fe and O is close to 1, namely, 0.83 with blowing and 1.5 without blowing. These values increase in the light regions up to 3.7 and 32, respectively. The value obtained on the wear track produced without blowing (3.7) is so low probably due to the fact that, in that case, dark spots

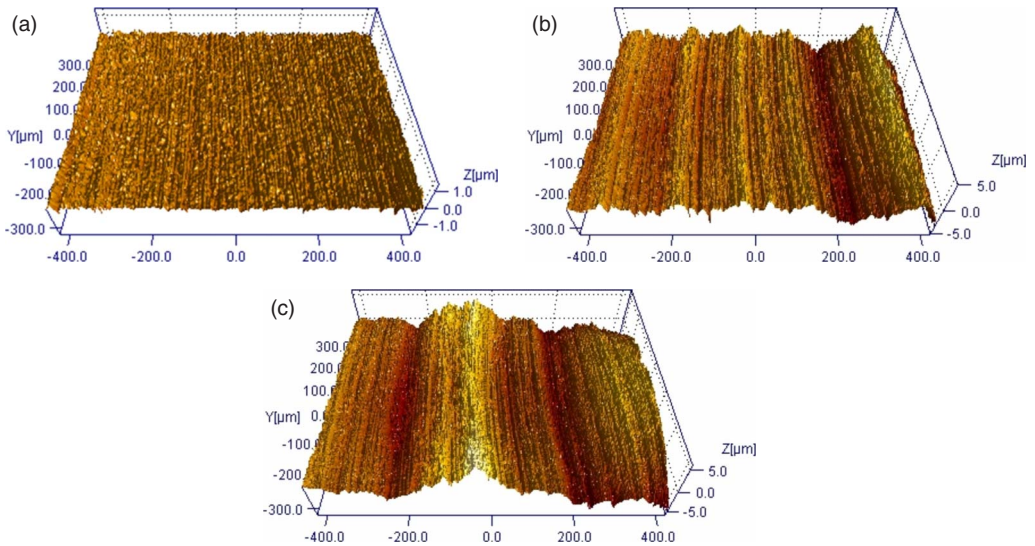

FIG. 12. (Color online) Three-dimensional images obtained by means of interferometric microscopy of the untested polished surface (upper) and of the wear track produced in sliding friction experiments carried out with (middle) and without (lower) blowing.

TABLE II. Values of parameters used to characterize the surface roughness (arithmetical mean deviation S_a, root-mean-square deviation S_q, skewness S_{sk}, and kurtosis S_{ku}) for the untested sample (UnS) surface and for the wear track (WT) produced in experiments carried out with blowing (WT-B) or without blowing (WT-NB) wear debris.

Sample	S_a	S_q	S_{sk}	S_{ku}
UnS	0.067	0.093	−1.77	17.9
WT-B	1.27	1.60	0.27	2.90
WT-NB	0.86	1.11	−0.097	3.48

are very close to each other. Anyhow, these results prove that the observed dark spots surely are iron oxides.

APPENDIX B: SURFACE ROUGHNESS OF UNTESTED SURFACE AND OF THE WEAR TRACK

Here we discuss surface roughness results for the sample before the wear test was carried out and for the wear track produced either with or without debris blowing (after 2000 m testing). Results were obtained by means of interferometric microscopy. Testing is carried out at the Laboratories of Alcan Europe in Alicante and is presented as (1) a low magnification overall three-dimensional (3D) view of the surface (see Fig. 12) and (2) quantitative values of S_a (arithmetical mean deviation) S_q (root-mean-square slope), S_{sk} (skewness), and S_{ku} (kurtosis of profile) are reported in Table II. An obvious result is that roughness, as characterized by S_a, is much higher in the wear track than in the untested surface: compare S_a=0.067 nm in the untested surface to S_a=0.856 and 1.27 nm in the wear track without and with debris blowing, respectively. The same parameter reveals a higher roughness in the wear track produced with blowing. Exactly, the same trend is followed by the root-mean-square deviation S_q. The skewness S_{sk}, on the other hand, is negative for the untested surface, something characteristic of grinded and polished surfaces. Again this parameter gives some difference between the tracks obtained with or without blowing, as S_{sk} is positive for the former and negative for the latter. Finally, kurtosis values greater than 3 denote peaked Gaussian height distributions, whereas for $S_{ku}<3$, the height distribution becomes broader. Again, the results reported in Table II are consistent with other data and with what one may have expected. The largest value of kurtosis corresponds to the untested sample, indicating a very narrow Gaussian height distribution. S_{ku} is around 3 for the wear track, being smaller (2.90) in the case of no blowing, in line with the rest of roughness parameters analyzed here and with the 3D profiles shown in Fig. 12. Specifically, while the untested surface has a rather flat profile, it becomes much more intricate in the wear track, being steeper in the wear track produced with debris blowing. In the latter case, the profile shown in Fig. 12 reveals a large amplitude long-wavelength oscillation, which is a consequence of the more intensive and less uniform wearing that occurs under debris blowing. The surface is much noisier at a small scale in the case without blowing, probably due to the many debris particles stuck on the track surface observed by means of SEM and optical microscopy. Finally, it is noted that debris accumulation near the track edges (which is likely to occur when the track is sufficiently deep) is surely the cause of the profile maxima observed in those regions for tracks produced either with or without debris blowing.

[1] B. N. J. Persson, Surf. Sci. Rep. **33**, 83 (1999).
[2] E. Rabinowicz, *Friction and Wear of Materials* (John Wiley & Sons, New York, 1995).
[3] F. P. Bowden and D. Tabor, *Friction and Lubrication of Solids, Parts I and II* (Oxford University Press, Oxford, 1954).
[4] F. Heslot, T. Baumberger, B. Perrin, B. Caroli, and C. Caroli, Phys. Rev. E **49**, 4973 (1994).
[5] F. R. Zypman, J. Ferrante, M. Jansen, K. Scanlon, and P. Abel, J. Phys.: Condens. Matter **15**, L191 (2003).
[6] S. V. Buldyrev, J. Ferrante, and F. R. Zypman, Phys. Rev. E **74**, 066110 (2006).
[7] M. Duarte, J. M. Molina, R. Prieto, E. Louis, and J. Narciso, TMS Annual Meeting 2006 (The Minerals , Metals, and Materials Society, San Antonio, 2006), pp. 247–250.
[8] M. Duarte, J. M. Molina, R. Prieto, E. Louis, and J. Narciso, Metall. Mater. Trans. A **38**, 298 (2007).
[9] M. Duarte, I. Vragovic, J. M. Molina, R. Prieto, J. Narciso, and E. Louis, Phys. Rev. Lett. **102**, 045501 (2009).
[10] R. Hallgass, V. Loreto, O. Mazzella, G. Paladin, and L. Pietronero, Phys. Rev. E **56**, 1346 (1997).
[11] F. Slanina, Phys. Rev. E **59**, 3947 (1999).
[12] D. L. Turcotte, Rep. Prog. Phys. **62**, 1377 (1999).
[13] S. A. Zaitsev, Physica A **189**, 411 (1992).
[14] N. P. Suh, *Tribophysics* (Prentice Hall, New Jersey, 1986).
[15] H. K. Lee, S. S. Kim, and D. G. Lee, Compos. Struct. **74**, 136 (2006).
[16] R. K. Uyyuru, M. K. Surappa, and S. Brusethaug, Wear **260**, 1248 (2006).
[17] F. H. Stott, Tribol. Int. **35**, 489 (2002).
[18] J. Jiang, F. H. Stott, and M. M. Stack, Tribol. Int. **31**, 245 (1998).
[19] J. Davidsen and H. G. Schuster, Phys. Rev. E **62**, 6111 (2000).
[20] P. Bak, C. Tang, and K. Wiesenfeld, Phys. Rev. A **38**, 364 (1988).
[21] L. P. Kadanoff, S. R. Nagel, L. Wu, and Su-min Zhou, Phys. Rev. A **39**, 6524 (1989).
[22] S. S. Manna, J. Phys. A **24**, L363 (1991).
[23] L. Laurson, M. J. Alava, and S. Zappieri, J. Stat. Mech.: Theory Exp. (2005), L11001.